

First-Order Statistics of Pulsed-Sinusoid Backscatter from Random Media: Basic Elements of an Exact Treatment

Larry Clifford Gilman

Abstract—In ultrasonic imaging systems, the instantaneous pressure at the transducer face during echo reception is typically comprised of many superimposed reflections of a pulse resembling an amplitude-modulated sinusoid. Generally, these reflections are randomly shifted in phase and randomly scaled in amplitude. Moreover, each reflected pulse may have been distorted by passage through a nonuniform medium.

The first-order amplitude statistics of such a waveform have long been considered of interest. The backscatter formation process has often been modeled as a random walk in two dimensions. For simplicity, the effects of amplitude-phase dependence and scatterer size distribution have not been fully included in previous work. In most cases of interest this is physically justified; but, given a strongly non-Rayleigh random medium, experience has shown that more accurate expressions may be required.

This paper points to the essentials of such an improved analysis. The effects of pulse structure and scatterer size distribution on the statistical properties of the individual step of the random walk are considered *de novo*. Simulation results are described.

I. INTRODUCTION

THE INSTANTANEOUS ACOUSTIC PRESSURE at a transducer face during echo reception is typically comprised of many superimposed reflections of an interrogating pulse. These reflections may be randomly shifted in phase and scaled in amplitude and, moreover, may be distorted during their passage through the insonified medium [1]–[3].

The first-order amplitude statistics of such waveforms have long been of interest [2], [4]–[6]. In particular, the instantaneous resultant of a sum of randomly scaled and phase-shifted sinusoidal pulses has often been modeled as a two-dimensional random walk [7]–[11]. The K distribution has been widely discussed as a descriptor of the amplitude distribution of such a walk (e.g., [7]–[10]) and has been found to supply a *relatively* good fit to the first-order envelope amplitude distribution of backscatter from human and canine myocardium (heart muscle), strongly non-Rayleigh scattering media [4]. However, even the K distribution often fails to fit such data well. This may be due to the fact that certain complicating factors have been traditionally ignored for the sake of analytic simplicity (e.g., the inherent amplitude-phase dependence of pulsed sinu-

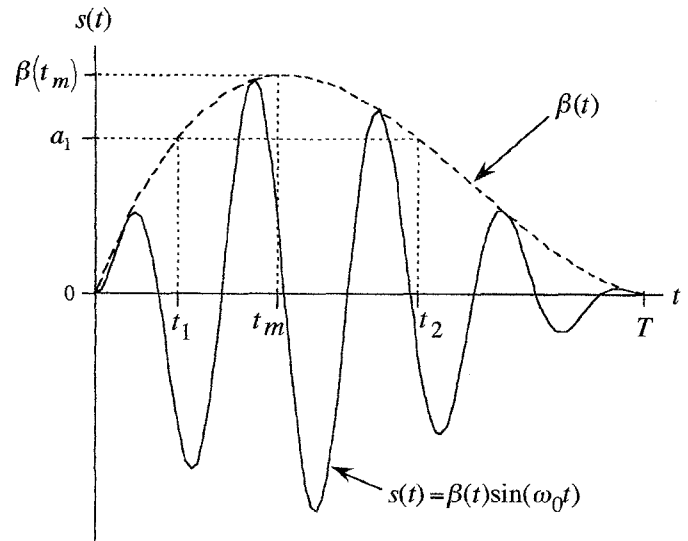


Fig. 1. Sketch of a typical sinusoidal pulse of duration T . $\beta(t)$ is the modulating function of the pulse envelope. Note that t_m is the time at which $\beta(t)$ is maximum, and that t_1 and t_2 are the roots of $a_1 - \beta(t) = 0$.

soids, and scatterer spacing and sizing). Such simplifications have often proved appropriate, but accurate characterization of backscatter from some non-Rayleigh random media may require an improved description of the backscatter formation process [4], [12].

Below, the effects of pulse structure and scatterer size on the statistical properties of the individual random step are considered. First, the analytic context of this paper is described (Section II). Second, the fundamental statistical properties of the individual random step are investigated (Section III). Third, the significance of the expressions given in Section III is discussed (Section IV).

II. RANDOM WALK REPRESENTATION OF THE BACKSCATTER FORMATION PROCESS

The pulse emitted by a wideband ultrasonic transducer usually resembles the amplitude-modulated sinusoid $s(t)$ shown in Fig. 1. Irregularities in an insonified random medium return numerous overlapping reflections of this pulse to the transducer. The resulting backscatter signal resembles a sinusoid amplitude-modulated by a bandlimited, noiselike quantity.

Manuscript received April 28, 1996; accepted February 18, 1997.
The author can be reached at 1649 Touhy Avenue, Apt. # 1-South, Chicago, IL 60626 (e-mail: psg720@nwu.edu).

If the backscatter echo envelope is “sampled” (i.e., averaged over a time interval very short relative to the center frequency of the signal), it is possible to treat the echo formation process as a two-dimensional random walk.

Such samples should be separated widely enough in time to be statistically independent, for samples which are closer together than the effective duration of a single pulse may share contributions from the same scatterers and thus be correlated [15]. Sufficiently isolated samples, however, can be conceptualized as outcomes of *independent* random walks.

The instantaneous contribution of a single reflected pulse can be modeled as a single complex vector step \mathbf{a}_j in a two-dimensional random walk commonly symbolized as follows:

$$\mathbf{A} = \sum_{j=1}^N \mathbf{a}_j. \quad (1)$$

In (1), \mathbf{A} and \mathbf{a}_j may be interpreted as complex vector representations of ideal sinusoids; N specifies the number of steps in the random walk, and $\mathbf{a}_j = a_j e^{i\phi_j}$. It is standard to assume independent a_j and ϕ_j and uniformly distributed ϕ_j . Furthermore, if all \mathbf{a}_j are equally well described by a single probability density function (PDF) $p_{\mathbf{a}}(\mathbf{a})$, then all subscripts may be dropped, i.e., $\mathbf{a}_j = \mathbf{a}$, $a_j = a$, and $\phi_j = \phi$.

If it is assumed that all \mathbf{a}_j are equivalent and independent and that ϕ is uniformly distributed on $[0, 2\pi]$, it can be shown that the PDF of $A = |\mathbf{A}|$ is

$$p_A(A) = 2\pi A p_{\mathbf{A}}(\mathbf{A}) = A \int_0^{\infty} u J_0(uA) \langle J_0(ua) \rangle^N du, \quad (2)$$

where $\langle J_0(ua) \rangle = \int_0^{\infty} J_0(ua) p_a(a) da$ and $J_0(\cdot)$ is the 0th-order Bessel function of the first kind [8], [11]. Note that in (2) $p_A(A)$ is a function of A only (isotropic); this follows from assuming independent \mathbf{a} and uniform ϕ .

Equation (2) was first offered by J. C. Kluver in 1905, has been frequently cited ever since, and is perfectly general for two-dimensional random walks with uniform angular distribution and independent, identically distributed steps. It is notably intractable; no closed-form general solution of (2) is available for $N > 3$ [11]. However, other expressions for $p_A(A)$ may be obtained by means of the same techniques which yield (2), if various assumptions, approximations, and limiting operations are applied. For example, the Rayleigh, Rician, and K distributions for $p_A(A)$, all of which have been used to describe ultrasonic backscatter, may be so derived [4], [5], [17].

However, the amplitude and angle (a and ϕ) of a random vector representing a sample of a pulsed sinusoid are not actually independent (Section III), and so the Kluver equation (2) cannot strictly describe the amplitude distribution of a random walk comprised of such vectors. In some situations of physical interest, such dependencies may have a significant effect on signal statistics, and in

such cases neither the general Kluver equation nor any of its special analytic solutions (PDFs such as the Rayleigh, K , etc.) will apply. Therefore, the elements of a more accurate random walk model may be useful. These are indicated below.

III. THE PDF OF SAMPLES OF THE ENVELOPE OF A SINGLE PULSE

A. Basic Terms

Consider a single pulse of finite duration T (Fig. 1). This pulse can be idealized as a sinusoidal carrier modulated by an envelope function $\beta(t)$:

$$s(t) = \beta(t) \sin(\omega_0 t) \quad (3)$$

Let n be the number of carrier periods modulated, not necessarily an integer. Scaling and delay of this single pulse by a randomly sized and located scatterer followed by sampling of the backscattered pulse at some instant of time can be thought of as a random experiment having as its outcome a two-dimensional phasor \mathbf{a} with amplitude a (corresponding to the instantaneous envelope magnitude) and phase $\phi = \omega_0 t$.

Below, the amplitude of the unscaled sample is labeled a_1 to distinguish it from that of the randomly scaled sample, a . Scaling can be thought of as occurring after sampling without loss of generality. Section III.B derives the marginal density $p_{a_1}(a_1)$; Section III.C derives the joint density $p_{a_1, \phi}(a_1, \phi)$; Section III.D examines the effect of multiple carrier periods per pulse on $p_{a_1, \phi}(a_1, \phi)$; Section III.E notes the effect of multiple carrier periods on the marginal density $p_{\phi}(\phi)$; and Sections III.F and III.G extend these results to the randomly scaled amplitude a .

B. The Marginal Density of the Unscaled Amplitude a_1

Let t be a randomly chosen time on the interval $[0, T]$. Let a_1 and ϕ be the pulse envelope amplitude and carrier phase, respectively, at time t . The PDF of a_1 depends on $\beta(t)$ and on the PDF of t as follows.

In this paper the pulse function $\beta(t)$ is defined as a smooth positive function possessing a single maximum at some t_m on the interval $[0, T]$ and equal to zero at its endpoints. Given such a $\beta(t)$, $a_1 - \beta(t) = 0$ possesses two real roots, t_1 and t_2 , on the interval $[0, T]$ (Fig. 1). If $p_t(t)$ is the PDF of t , then by Papoulis [18] it follows that

$$p_{a_1}(a_1) = \frac{p_t(t_1)}{|\beta'(t_1)|} + \frac{p_t(t_2)}{|\beta'(t_2)|}, \quad (4)$$

where $\beta'(t) = \frac{d}{dt} \beta(t)$ and $p_{a_1}(a_1)$ is defined on $0 \leq a_1 \leq \beta(t_m)$.

The beta function $\beta_{(m,k)}(t)$ provides an illustrative $\beta(t)$. For positive integers m and k , with $k > 1$ and $m > k$,

$$\beta_{(m,k)}(t) = \frac{(m+1)!}{k!(m-k)!} t^k (1-t)^{m-k} \text{ for } 0 \leq t \leq 1. \quad (5)$$

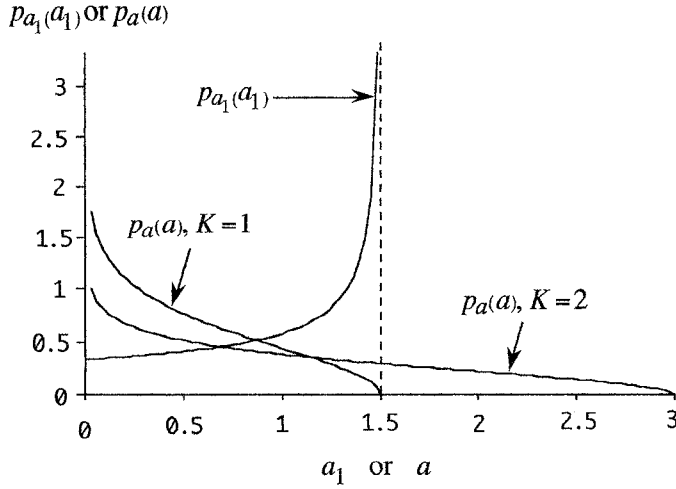


Fig. 2. See Sections III.B and III.F. Shown are (a) $p_{a_1}(a_1)$ for the beta pulse $\beta_{(2,1)}(t)$ with $n = 1$ and (b) $p_a(a)$, where $a = a_1 a_2$, a_1 is as above, and a_2 is uniformly distributed on $[0, K]$. $p_a(a)$ is shown for two values of K .

For all valid (m, k) , $\beta_{(m,k)}(t)$ has a pulselike character; the illustrative $\beta(t)$ plotted in Fig. 1 is $\beta_{(3,1)}(t)$. Unlike the Gaussian pulse often used in backscatter simulations [19], $\beta_{(m,k)}(t)$ is nonzero only on $[0, 1]$, so the range of t need not be arbitrarily restricted to prevent the PDF of a_1 from being completely concentrated at $a_1 = 0$.

In particular, the parabolic beta pulse $\beta_{(2,1)}(t)$ may be used for illustrative purposes:

$$\beta_{(2,1)}(t) = 6t(1-t) \text{ for } 0 \leq t \leq 1. \quad (6)$$

With t uniform on $[0, 1]$, $p_t(t) = 1$ for all t . Substituting for all terms in (4), $p_{a_1}(a_1)$ is found for this example (Fig. 2):

$$p_{a_1}(a_1) = (9 - 6a_1)^{-1/2} \text{ for } 0 \leq a_1 \leq \frac{3}{2}. \quad (7)$$

Equation (7) and Fig. 2 illustrate the character of a random variable consisting of envelope samples from a single pulse. At every value of a_1 where the derivative of $\beta(t)$ equals zero, $p_{a_1}(a_1)$ goes to infinity.

C. The Joint Density of Amplitude a_1 and Phase ϕ

The case where precisely one period of the carrier is modulated ($n = 1$) is considered in this section; this result generalizes straightforwardly to the multiple-period case (next section).

The joint density $p_{a_1, \phi}(a_1, \phi)$ is sought and $p_{a_1}(a_1)$, $p_\phi(\phi)$, and the domain of $p_{a_1, \phi}(a_1, \phi)$ are known; $p_{a_1}(a_1)$ is given by (4), $P_\phi(\phi)$ is defined for $0 \leq \phi \leq 2\pi$, and the domain of $p_{a_1, \phi}(a_1, \phi)$ consists of all points on the curve $a_1 = \beta\left(\frac{\phi T}{2\pi}\right)$. Application of basic theorems of probability

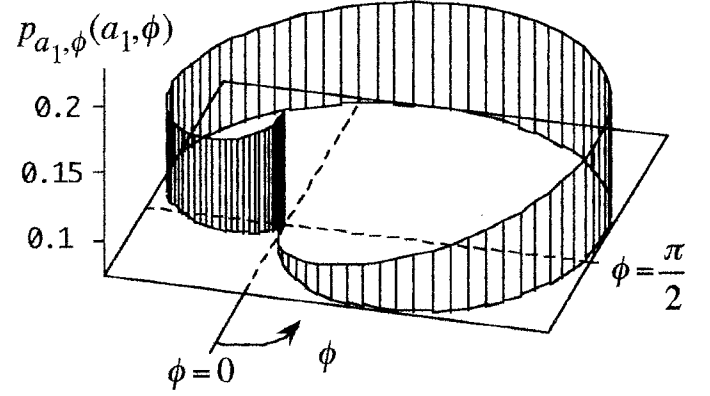


Fig. 3. See Section III.C. Shown is $p_{a_1, \phi}(a_1, \phi)$ for the beta pulse $\beta_{(3,1)}(t)$ with $n = 1$, in cylindrical coordinates. Radial coordinate is a_1 .

and the calculus shows that

$$p_{a_1, \phi}(a_1, \phi) = p_\phi(\phi) \left\{ \left[\beta' \left(\frac{\phi T}{2\pi} \right) \frac{T}{2\pi} \right]^2 + 1 \right\}^{-1/2} \quad (8)$$

for $0 \leq \phi \leq 2\pi$, $a_1 = \beta\left(\frac{\phi T}{2\pi}\right)$.

The beta pulse $\beta_{(3,1)}(t)$ provides an example (Fig. 3). For this pulse shape and ϕ uniform,

$$p_{a_1, \phi}(a_1, \phi) = \left[\left(12 - \frac{24\phi}{\pi} + \frac{9\phi^2}{\pi^2} \right)^2 + (2\pi)^2 \right]^{-1/2} \quad (9)$$

for $0 \leq \phi \leq 2\pi$, $a_1 = \frac{6\phi}{\pi} \left(1 - \frac{\phi}{2\pi} \right)^2$.

Note that for a pulse comprised of a single modulated carrier period, amplitude is a simple function of phase: $a_1 = \beta\left(\frac{\phi}{\omega_0 T}\right)$ for $0 \leq \phi \leq \omega_0 T$. This contrasts with the amplitude-phase *independence* almost universally assumed for the steps of the random walk. In other words, vectors that symbolize samples of pulsed sinusoids intrinsically violate one of the assumptions supporting the classic random walk model. This may account for the occasional inadequacy of predictions based on variants of the classic model.

D. The Effect on $p_{a_1, \phi}(a_1, \phi)$ of $n > 1$

The multiperiod ($n > 1$) case follows as a straightforward generalization of the single-period ($n = 1$) case.

Let $T = \frac{n2\pi}{\omega_0}$, where n is some number greater than 1, not necessarily integer. Since the phase argument of a two-dimensional vector can only range meaningfully between 0 and 2π , distinction is now made between $\Phi = \omega_0 t$, the "absolute phase" having PDF $p_\Phi(\Phi)$ which can range from 0 to ∞ , and ϕ , the "cyclic phase" having PDF $p_\phi(\phi)$ which can range from 0 to 2π . Clearly, $\phi = \Phi \bmod 2\pi$.

Equation (8) holds directly for $p_{a_1, \Phi}(a_1, \Phi)$ with $n > 1$,

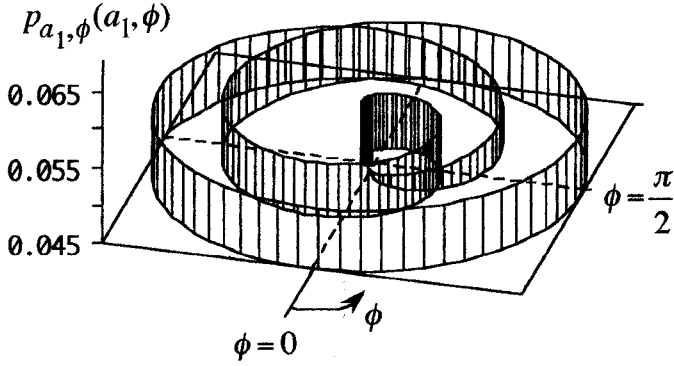


Fig. 4. See Section III.D. Shown is $p_{a_1, \phi}(a_1, \phi)$ for $\beta_{(3,1)}(t)$ with $n = 3$, in cylindrical coordinates. Radial coordinate is a_1 .

given appropriate changes in argument and range:

$$p_{a_1, \Phi}(a_1, \Phi) = p_{\Phi}(\Phi) \left\{ \left[\beta' \left(\frac{\Phi}{\omega_0} \right) \frac{1}{\omega_0} \right]^2 + 1 \right\}^{-1/2}$$

$$\text{for } 0 \leq \Phi \leq \omega_0 T, a_1 = \beta \left(\frac{\Phi}{\omega_0} \right). \quad (10)$$

The equivalent result in terms of cyclic phase ϕ is readily found. For all $0 \leq \phi \leq 2\pi$, all integers i such that $\phi + i2\pi \leq \omega_0 T$, and all $a_1 = \beta \left(\frac{\phi + i2\pi}{\omega_0} \right)$,

$$p_{a_1, \phi}(a_1, \phi) = \sum_i \left(p_{\phi}(\phi) \left\{ \left[\beta' \left(\frac{\phi + i2\pi}{\omega_0} \right) \frac{1}{\omega_0} \right]^2 + 1 \right\}^{-1/2} \right). \quad (11)$$

Note that the number of terms in (11) at any given point is not n (which may not even be an integer) but depends on a_1 and ϕ .

For increasing n , $p_{a_1, \phi}(a_1, \phi)$ becomes increasingly convoluted in appearance; in Fig. 4, $p_{a_1, \phi}(a_1, \phi)$ is plotted for the beta pulse $\beta_{(3,1)}(t)$ with $n = 3$. Compare with the $n = 1$ case (Fig. 3).

Each of the $p_{a_1, \phi}(a_1, \phi)$ considered in this section can be viewed as the PDF of a two-dimensional random walk only one step in length, the joint PDF of the phase and amplitude of this random vector being given by (11).

E. The Effect on $p_{\phi}(\phi)$ of $n > 1$

The effect on $p_{\phi}(\phi)$ of $n > 1$ remains to be remarked upon.

If a sinusoidal carrier of frequency ω_0 rad/sec is modulated by a pulse envelope of duration T comprising n carrier periods, then some integer number n_I of complete carrier periods will be contained in the pulse, plus some amount of "extra" phase Φ_E , where $0 < \Phi_E < 2\pi$. If one assumes Φ uniform on $[0, T]$ and defines $\Phi_T = \omega_0 T$, it is easy to show that

$$p_{\phi}(\phi) = \begin{cases} \frac{n_I + 1}{\Phi_T} & \text{for } 0 \leq \phi \leq \Phi_E \\ \frac{n_I}{\Phi_T} & \text{for } \Phi_E \leq \phi \leq 2\pi. \end{cases} \quad (12)$$

As n_I increases, the relative difference in amplitude of $p_{\phi}(\phi)$ for $0 \leq \phi \leq \Phi_E$ and for $\Phi_E < \phi \leq 2\pi$ decreases approximately as $\frac{1}{n_I}$; for large n the possible departure from uniformity of $p_{\phi}(\phi)$ is correspondingly small.

F. Scaling by a Random Multiplier

The scaling of a pulse reflection by a scatterer of random size can be idealized as multiplication of a_1 by a random variable a_2 with PDF $p_{a_2}(a_2)$ for $0 \leq a_2 \leq A_2$. The observed amplitude may then be defined as $a = a_1 a_2$ with PDF $p_a(a)$. The joint PDF of amplitude and phase, $p_{a, \phi}(a, \phi)$, is sought. The case of $n = 1$ is considered first.

By applying basic probability theory, the joint density of a and ϕ may be found in terms of $p_{\phi}(\phi)$, $p_{a_2}(\cdot)$, and $\beta(\cdot)$:

$$p_{a, \phi}(a, \phi) = p_{\phi}(\phi) \beta^{-1} \left(\frac{\phi T}{2\pi} \right) p_{a_2} \left(a \beta^{-1} \left[\frac{\phi T}{2\pi} \right] \right)$$

$$\text{for } 0 \leq \phi \leq 2\pi, \quad 0 \leq a \leq A_2 \beta \left(\frac{\phi T}{2\pi} \right). \quad (13)$$

Above, $\beta^{-1}(\cdot) = \frac{1}{\beta(\cdot)}$. Note that the range of a depends on ϕ . Equation (13) may be compared to (8).

An expression for the marginal density of a follows by integration of (13):

$$p_a(a) = \int_{\phi_1}^{\phi_2} p_{\phi}(\phi) \beta^{-1} \left(\frac{\phi T}{2\pi} \right) p_{a_2} \left(a \beta^{-1} \left[\frac{\phi T}{2\pi} \right] \right) d\phi$$

$$\text{for } 0 \leq a \leq A_2 \beta(t_m), \quad (14)$$

where ϕ_1 and ϕ_2 are functions of a only, being the roots of $a - A_2 \beta \left(\frac{\phi T}{2\pi} \right) = 0$. Equation (14) may be compared to (4), and gives $p_a(a)$ regardless of n .

In the illustrative case of the beta pulse $\beta_{(2,1)}(t)$ with a_2 uniform on $[0, K]$, (14) becomes:

$$p_a(a) = \frac{1}{3K} \ln \left[\frac{1 + \left(1 - \frac{2a}{3K}\right)^{1/2}}{1 - \left(1 - \frac{2a}{3K}\right)^{1/2}} \right] \text{ for } 0 \leq a \leq \frac{3K}{2}. \quad (15)$$

Equation (15) is plotted in Fig. 2 for $K = 1$ and $K = 2$ on the same scale as $p_{a_1}(a_1)$, the PDF of the unscaled random variable a_1 (7). The effect of randomly scaling a_1 is dramatic; small values of a are relatively more probable than are small values of a_1 , while $p_a(a)$ has an asymptote at $a = 0$ rather than at the upper end of its range.

G. The Effect on $p_{a, \phi}(a, \phi)$ of $n > 1$

Equation (13) holds for $n = 1$. If $n > 1$ then $p_{a, \phi}(a, \Phi)$ may be mapped to $p_{a, \phi}(a, \phi)$ as in Section III.D, where Φ and ϕ are the absolute and cyclic phase, respectively. For $0 \leq \phi \leq 2\pi$, all i such that $\phi + i2\pi \leq \omega_0 T$, and all

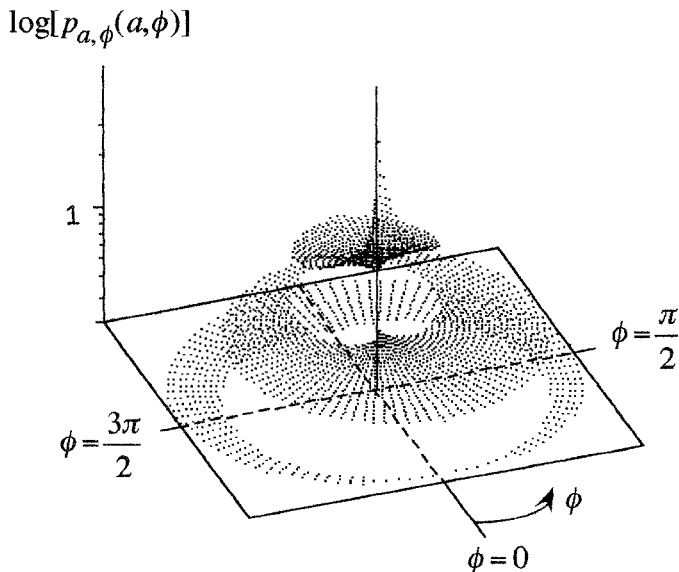


Fig. 5. See Section III.G. Shown is $p_{a,\phi}(a, \phi)$ for a $\beta_{(2,1)}(t)$ pulse with $n = 1$ and a_2 uniform on $[0, 1]$, in cylindrical coordinates. Radial coordinate is a_1 .

$$a \leq A_2 \beta\left(\frac{\phi + i2\pi}{\omega_0}\right),$$

$$p_{a,\phi}(a, \phi) = \sum_i \left\{ p_{\Phi}(\Phi) \Big|_{\Phi=\phi+i2\pi} \beta^{-1}\left(\frac{\phi + i2\pi}{\omega_0}\right) \times p_{a_2} \left[a \beta^{-1}\left(\frac{\phi + i2\pi}{\omega_0}\right) \right] \right\}. \quad (16)$$

Note that, as with (11), the number of terms in (16) at any point depends on a and ϕ .

Equation (16) expresses the statistical dependence of individual samples from a randomly scaled and shifted sinusoidal pulse on pulse shape, scaling, and phase. For the case of the beta pulse $\beta_{(2,1)}(t)$ with $n = 3$, uniform ϕ , and a_2 uniform on $[0, 1]$, (16) is plotted in Fig. 5.

It should be noted that as n increases, i.e., for $\omega_0 T \gg 1$, the whole range of cyclic carrier phase ϕ ($0 \rightarrow 2\pi$) will tend to be modulated by every infinitesimal segment of $\beta(t)$, so that every carrier phase can be associated with every possible amplitude. Thus a and ϕ tend towards independence with increasing n , i.e.:

$$\lim_{n \rightarrow \infty} p_{a,\phi}(a, \phi) = p_a(a) p_{\phi}(\phi), \quad (17)$$

where $p_a(a)$ is always given by (14).

For the case of the beta pulse $\beta_{(3,1)}(t)$ with $n = 15$, uniform ϕ , and a_2 uniform on $[0, 1]$, (16) is plotted in Fig. 6.

Note that, although evaluation of (16) does not require knowledge of the roots ϕ_1 and ϕ_2 , they are required for determining the bounds of integration for determination of $p_a(a)$ by (14). The roots ϕ_1 and ϕ_2 may not be explicitly available, while the integral in (14) may not have a closed-form solution even when ϕ_1 and ϕ_2 are known and the functional forms of $\beta(t)$ and $p_{a_2}(a_2)$ are relatively simple.

Finally, note that these results describe the statistical character of an individual random step. A typical random

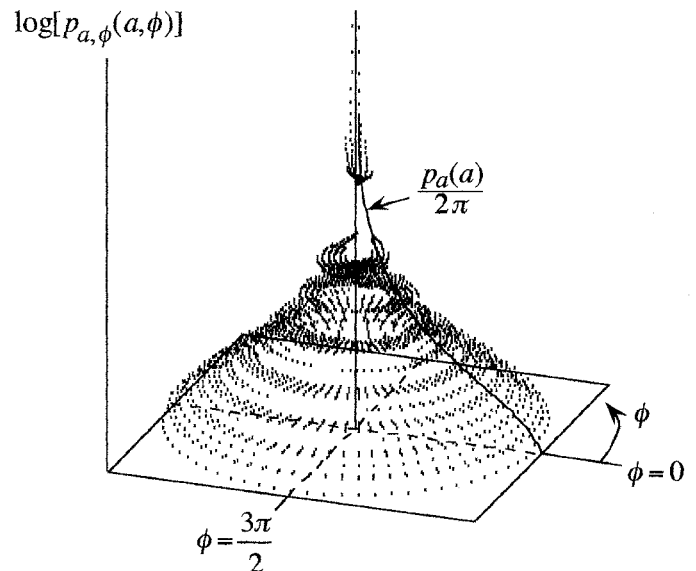


Fig. 6. See Section III.G. Shown is $p_{a,\phi}(a, \phi)$ for a $\beta_{(3,1)}(t)$ pulse with $n = 15$ and a_2 uniform on $[0, 1]$, in cylindrical coordinates. Radial coordinate is a_1 . To illustrate (17), the $n \rightarrow \infty$ distribution $\frac{p_a(a)}{2\pi}$ is also shown (for $\phi = 0$ only).

walk consists of N such steps where N is also a random variable with PDF $p_N(N)$ (often modeled as Poisson). The PDF of \mathbf{A} (1) is the inverse two-dimensional Fourier transform of the characteristic function of \mathbf{A} (i.e., the term in square brackets below):

$$p_{\mathbf{A}}(\mathbf{A}) = \frac{1}{4\pi^2} \int \left[\sum_{N=0}^{\infty} p_N(N) \left\{ \int_{\phi} \int_a e^{-i\mathbf{u} \cdot \mathbf{A}} \times p_{a,\phi}(a, \phi) da d\phi \right\}^N \right] e^{-i\mathbf{u} \cdot \mathbf{A}} d\mathbf{u}. \quad (18)$$

In (18), the integration with respect to a is from 0 to the ϕ -dependent boundary of the domain of $p_{a,\phi}(a, \phi)$, and that with respect to ϕ is from 0 to 2π . Under the simplifying assumptions of ϕ uniform and independent and N constant, (18) is equivalent to the Kluver equation (2). In all cases (14) gives $p_a(a)$ for a random walk fundamentally governed by randomly shifted and scaled sinusoidal pulses. Numerical methods are required to evaluate either (2) or (18) for nontrivial cases.

IV. SIMULATION

The expressions for $p_a(a)$ and $p_{a,\phi}(a, \phi)$ given in Sections III.F and III.G are, despite the simplicity of their derivation, not generally amenable to analytic solution. They are offered here specifically to suggest a starting point for very realistic numerical modeling of backscatter from unruly random media (e.g., myocardium, intravascular plaque) that possesses envelope statistics not adequately described by more parsimonious, tractable, and

familiar models (such as those that predict the Rayleigh, Rician, K , and kindred PDFs).

Heuristic Monte Carlo simulation has shown that pulse shape, the PDF of the random scaling variable a_2 , and (a, ϕ) dependence can all contribute measurably to the statistical character of the envelope PDF $p_a(a)$ under assumptions realistic for such media [5].

A series of random walks may be easily simulated by iterating the following procedure M times (where M is made large enough to yield stable results):

- I) A number N is chosen from a Poisson-distributed process.
- II) N random steps $\mathbf{a}_j = a_j e^{i\phi_j}$ are created, each as follows:
 - (A) A phase ϕ_j is chosen uniformly on $[0, 2\pi]$.
 - (B) An amplitude a_j is chosen by one of the following two alternative methods:

- 1) Any chosen carrier phase ϕ_j recurs either n_I or $n_I + 1$ times in a single pulse (see Fig. 1, for example, where $n_I = 4$). From among the n_I or $n_I + 1$ corresponding time values, one is chosen at random ($t = t_j$) and $(a_1)_j$ is set equal to $\beta(t_j)$. A value for $(a_2)_j$ is then chosen according to a specific $p_{a_2}(a_2)$ (Section III.F) and a_j is set equal to $(a_1)_j(a_2)_j$. To simulate no random scaling, $(a_2)_j$ is set to unity.

- 2) Alternatively, an a_j may be selected independently of ϕ_j using the PDF $p_a(a)$ (4). If method 1) is used, then (a, ϕ) dependence is preserved; if method 2), then the influence of pulse shape on $p_a(a)$ is retained but not that of finite n_I on $p_{a,\phi}(a, \phi)$ (Section III.G).

- (C) The vector sum \mathbf{A} of all N steps is formed, and its amplitude A is calculated.

The M random walk amplitudes thus produced may be treated as simulated backscatter envelope samples (Section II). Their histogram may be compared to hypothetical PDFs via goodness-of-fit testing or other methods, and the effects of such factors as the pulse envelope shape $\beta(t)$, the PDF of the random multiplier a_2 , and the assumption of (a, ϕ) dependence may be examined.

In simulations conducted by the author, $p_{a_2}(a_2)$ was chosen to embody some of the complex character of myocardial scattering, which arises from at least three somewhat distinct, coextensive scatterer populations of widely differing character [5], [20]:

$$p_{a_2}(a_2) = \begin{cases} p_1 & \text{for } 0 \leq a_2 < K_1 \\ p_2 & \text{for } K_1 \leq a_2 < K_2 \\ p_3 & \text{for } K_2 \leq a_2 \leq K_3 \end{cases} \quad (19)$$

where the constants $(p_1, p_2, p_3; K_1, K_2, K_3)$ specify a piecewise uniform PDF. Typically, $p_1 \gg p_2 \gg p_3$ and $K_1 \gg K_2 \gg K_3$ to encode the relative frequencies of weak, moderate, and strong scatterers, respectively.

A realistic tissue backscatter model must reproduce the tendency of much actual tissue backscatter to be more or less K distributed [4], [21]. In particular, an $M = 1000$ simulation based on a $\beta_{(2,1)}(t)$ pulse with $n = 8$

and $(p_1, p_2, p_3; K_1, K_2, K_3) = (9.009, 0.048, 0.004; .1, 2., 5.)$ produces data that is K distributed with a chi square test significance of 0.760 (compared to significances of 0.113, 0.001, and $< .001$ for the Nakagami- m , Rician, and Rayleigh PDFs respectively).¹

The effect of (α, ϕ) dependence on envelope statistics is inevitably smaller for larger n (Section III.G) and is already slight at $n = 8$ for the conditions of this exemplary simulation; however, for $n \leq 6$ or so (a realistic range for some wideband pulses), (a, ϕ) dependence is increasingly influential. For example, holding all other factors constant in this simulation while setting $n = 2$, chi square significance declines to 0.558, 0.010, ≈ 0 , and ≈ 0 for the K , Nakagami- m , Rician, and Rayleigh PDFs, respectively.

Retaining $n = 8$ while changing the pulse shape to a more realistic-looking $\beta_{(5,1)}(t)$ has a similar effect but moves the observed statistics even farther from all the candidate distributions (e.g., significance for the K PDF declines from 0.760 to 0.172, and the rest even more drastically). Alterations in the $p_{a_2}(a_2)$ parameters also affect these results, but to explore all such variations would take this discussion far afield.

Similar goodness-of-fit order (i.e., K best, Nakagami- m second-best, etc.)—and an even greater range of absolute goodness of fit—has previously been observed for these four candidate PDFs using data obtained from myocardium *in vivo* and *in vitro* [4]. Note that although the K PDF is a better fit than three alternative PDFs under the exemplary range of conditions cited, it is not consistently impressive in absolute terms. There is room for significantly improved characterization of some backscatter data even given the usefulness of the K PDF.

The primary use of simulations like that described above is to demonstrate that retention of fundamental pulse-shape and phase dependencies such as are pointed out in Section III is justified in the analysis of wideband pulse backscatter from some random media.

V. CONCLUSIONS

Accurate understanding of the backscatter process is sought as an aid to tissue characterization; attempts to deduce tissue states from signal statistics are inevitably hampered by inadequate models of the backscatter process itself.

In clinical or laboratory environments other factors than those discussed above may further complicate the process of backscatter formation, e.g., phase distortion produced by irregularities in the insonified medium may affect signal statistics. In phased-array systems, the idea of a determinate $\beta(t)$ perfectly replicated in all transmission events is questionable. Frequency-dependent attenuation may significantly alter the character of pulses returned by more distant scatterers.

¹In order to conduct the chi square test, the amplitude range of the data was divided into 128 equal intervals and the data points were classed accordingly.

Further experimental and numerical investigation of the dependence of signal statistics on medium microstructure, pulse shape, and amplitude-phase dependence is called for. Such dependencies can be modeled using the expressions given here; their significance relative to other factors in realistic contexts remains to be investigated.

REFERENCES

- [1] K. Shung and D. Fei, "The stochastic nature of echoes from biological tissues," *IEEE Seventh Annu. Conf. Eng. Med. Biol. Soc.*; pp. 241-242, 1985.
- [2] R. Wagner, S. Smith, J. Sandrik, and H. Lopez, "Statistics of speckle in ultrasound B-scans," *IEEE Trans. Sonics Ultrason.*, vol. 30, no. 3, pp. 156-163, 1983.
- [3] E. Jakeman and P. Pusey, "Non-Gaussian fluctuations in electromagnetic radiation scattered by a random phase screen. I. Theory," *J. Physics A, Math. Gen.*, vol. 8, no. 3, pp. 369-391, 1975.
- [4] L. Clifford, P. Fitzgerald, and D. James, "Non-Rayleigh first-order statistics of ultrasonic backscatter from normal myocardium," *Ultras. Med. Biol.*, vol. 19, no. 6, pp. 487-495, 1993.
- [5] L. Clifford, "On the First-Order Amplitude Statistics of Myocardial Ultrasonic Backscatter," Ph.D. dissertation, Thayer School of Engineering, Dartmouth College, Hanover, NH, 1995.
- [6] R. Wagner, M. Insana, and D. Brown, "Statistical properties of radio-frequency and envelope-detected signals with applications to medical ultrasound," *J. Opt. Soc. Amer. A*, pp. 910-922, May 1987.
- [7] E. Jakeman, and P. Pusey, "A model for non-Rayleigh sea echo," *IEEE Trans. Antennas Propagat.*, vol. AP-24, pp. 806-814, 1976.
- [8] —, "Significance of K distributions in scattering experiments," *Phys. Rev. Lett.*, vol. 40, pp. 546-550, 1978.
- [9] E. Jakeman and R. Tough, "Generalized K distribution: a statistical model for weak scattering," *J. Acoust. Soc. Amer. A*, vol. 4, no. 9, pp. 1764-1772, 1987.
- [10] L. Weng, J. Reid, P. Shankar, and K. Soetanto, "Ultrasound speckle analysis based on the K -distribution," *J. Acoust. Soc. Amer.*, vol. 89, pp. 2992-2995, 1991.
- [11] K. Pearson, "A mathematical theory of random migration," *Drapers' Company Research Memoirs, Biometric Series*, Dulau & Co., London: 1906, pp. 3-60.
- [12] J. Hampshire, II, "A Non-Rayleigh Model for Ultrasonic Backscatter from Myocardium," Master's thesis, Thayer School of Engineering, Dartmouth College, Hanover, NH, 1988.
- [13] J. Rayleigh, "On the problem of random vibrations, and of random flights in one, two, or three dimensions," *London, Edinburgh, and Dublin Philosophical Magazine J. Sci.*, vol. 37, pp. 321-347, 1919.
- [14] M. Teich and P. Diament, "Multiply stochastic representations for K distributions and their Poisson transforms," *J. Opt. Soc. Amer. A*, vol. 6, pp. 80-91, 1989.
- [15] P. He and J. Greenleaf, "Application of stochastic analysis to ultrasonic echoes—estimation of attenuation and tissue heterogeneity from peaks of echo envelope," *J. Acoust. Soc. Amer.*, vol. 19, pp. 526-534, 1986.
- [16] T. Tuthill, R. Sperry, and K. Parker, "Deviations from Rayleigh statistics in ultrasonic speckle," *Ultrason. Imag.*, vol. 10, pp. 81-89, 1988.
- [17] K. Shung, R. Sigelmann, and J. Reid, "Scattering of ultrasound by blood," *IEEE Trans. Biomed. Eng.*, vol. BME-23, no. 6, pp. 460-467, 1976.
- [18] A. Papoulis, *Probability, Random Variables, and Stochastic Processes*, McGraw-Hill, New York, 1984.
- [19] F. Barber and M. Goodsitt, "Digital simulation of pulsed ultrasonic waveforms," *Ultrason. Imag.*, vol. 1, pp. 303-324, 1979.
- [20] J. Caulfield and T. Borg, "The collagen network of the heart," *Lab. Invest.*, vol. 40, no. 3, pp. 364-372, 1979.
- [21] P. Shankar, "A model for ultrasonic scattering from tissues based on the K distribution," *Phys. Med. Biol.*, vol. 40, pp. 1633-1649, 1995.

Larry C. Gilman received a B.S. in Electrical Engineering from the Rutgers College of Engineering in 1984, an M.S.E.E. from Lehigh University in 1985, and a Ph.D. in Electrical Engineering from the Thayer School of Engineering, Dartmouth College, in 1996. There he studied the statistical properties of cardiac ultrasound under the advisorship of Dr. Douglas James, M.D., at the Dartmouth-Hitchcock Medical Center.